South African Journal of Chemical Engineering 41 (2022) 43–50

Contents lists available at ScienceDirect

South African Journal of Chemical Engineering

journal homepage: www.elsevier.com/locate/sajce

Efficient hydrogen production by microwave-assisted catalysis for glycerol-water solutions via NiO/zeolite-CaO catalyst

Husni Husin [a,b,*], Erdiwansyah Erdiwansyah [b,e], Ahmadi Ahmadi [a], Fahrizal Nasution [b], Wahyu Rinaldi [a], Faisal Abnisa [c], Rizalman Mamat [d]

[a] Reaction Engineering and Catalysis Laboratory, Department of Chemical Engineering, Faculty of Engineering, Universitas Syiah Kuala, Jl. Tgk. Syech Abdurrauf No.7 Darussalam Banda Aceh 23111, Indonesia
[b] Doctoral Program, School of Engineering, Universitas Syiah Kuala, Darussalam Banda Aceh, 23111 Indonesia
[c] Department of Chemical and Materials Engineering, Faculty of Engineering, King Abdulaziz University, Rabigh, 21911, Saudi Arabia
[d] Mechanical Engineering, Universiti Malaysia Pahang, 26600 Pekan, Pahang, Malaysia
[e] Faculty of Engineering, Universitas Serambi Mekkah, Banda Aceh 23245, Indonesia

ARTICLE INFO

Keywords:
Nickel
Calcium oxide
Microwave irradiation
Hydrogen production

ABSTRACT

Hydrogen from glycerol is one of the most potent green energy sources to replace fossil fuels. Thus, converting a glycerol solution to hydrogen through microwave-assisted catalysis is continuously gaining interest from researchers worldwide. The research aim was to combine NiO/zeolite and CaO for efficient hydrogen production from glycerol-water solution via microwave-assisted. The BET, XRD, and TEM were applied to characterize the properties of the NiO/zeolite-CaO catalyst. The influence of CaO content on NiO/zeolite (NiO/zeolite-CaO) catalyst, and microwave power on glycerol-water decomposition into hydrogen were investigated systematically. The catalytic performance for hydrogen production from glycerol-water solution was conducted in a fixed bed quartz-tube flow reactor via microwave irradiation a fed flow-rate (FFR) of 0.5 ml/min. Several characteristics, such as heating rate of 300–600 W, have been studied, CaO content of 10 wt.%, 30 wt.%, 40 wt.%, 50 wt.%, 60 wt.%, and 100 wt.%, respectively. The combined utilization of NiO/zeolite and CaO was efficient in obtaining more hydrogen production. Furthermore, the maximum conversion was found to be around 98.8%, while the highest hydrogen purity was found to be up to 96.6% when 20 wt.% NiO was used as an active site on natural zeolite and 50 wt.% CaO was used.

1. Introduction

Environmentally friendly energy has become a very important concern for industry and society globally (Macedo et al., 2019; Zhao et al., 2018). Energy sourced from fossil fuels is still the mainstay for the industry today (Aparamarta et al., 2020; Can and Yildirim, 20190). The problem of increasing environmental pollution and decreasing energy reserves has become a concern for scientists to look for alternative energy sources (Kasirajan, 2021; Sy et al., 2019). The search for alternative energy aims to replace depleting fossil fuels (Abdel-Basset et al., 2021; Hani et al., 2018). One of the efforts that can be done to deal with energy shortages is to utilize alternative energy from renewable energy sources that are friendly to the environment (Al Bacha et al., 2021; Husin et al., 2018).

Clean and renewable energy sources such as hydrogen using energy alternative to replace fossil fuels (Mardian et al., 2018; Koc and Avci, 2017). Hydrogen energy is secondary energy that can be converted into heating energy, especially for electricity through the combustion process (Husin et al., 2014; Baloyi et al., 2016). Thus, the interest in sourcing hydrogen raw materials from renewable and sustainable sources is increasing (Khodabandehloo et al., 2020; Zou et al., 2018). The utilization of renewable sources of methanol (Aparamarta et al., 2020; Husin et al., 2011a) and ethanol (Sharma et al., 2017) have been investigated by several researchers. However, the production of H_2 has still been constrained by the chemical reaction's thermodynamic equilibrium (Wang et al., 2011) and the highest H_2 generated is generally 50% (Widyawati et al., 2011). Glycerol is a by-product of biodiesel production, with its high source of 10 wt.% can be used as a renewable source (Ribao et al., 2019; H. Husin et al., 2017). It has emerged as a possible raw material for hydrogen synthesis (Moran et al., 2020).

* Corresponding author.
E-mail address: husni_husin@che.unsyiah.ac.id (H. Husin).

https://doi.org/10.1016/j.sajce.2022.04.004
Received 3 December 2021; Received in revised form 4 March 2022; Accepted 29 April 2022
Available online 1 May 2022

Various processes to degrade glycerol and biomass to hydrogen have been reported, especially the steam reforming process (Qingli et al., 2021), microwave heating (Czylkowski et al., 2016), syngas (Lin, 2013), photocatalytic (Sui et al., 2020), and glycerol steam reforming (GSR) (Tamošiūnas et al., 2017). The steam reforming produces 7 mol of hydrogen and 3 mol CO_2 per mole of glycerol involved in the reaction according to the degradation reactions of glycerol as follows:

Gas products:

$$C_3H_8O_3 + 3H_2O \rightarrow 7H_2 + 3CO_2 \quad (1)$$

One of the difficulties in using glycerol through the steam reforming process is to produce a high CO_2 content (Wang et al., 2011). Therefore, it is necessary to find a better way to produce high purity hydrogen from renewable sources. The acceleration of the reaction in a very promising catalytic area can be done by applying the microwave irradiation method by combining it with the NiO catalyst and CaO as CO_2 sorption. Irradiation with microwaves can reduce response from hours to minutes. The electric field and catalyst generate a quick rise in temperature due to the dipole's rapid rotation during the heating process is the key to a rapid increase in chemical reaction rates when employing microwaves (Chehade et al., 2020; Parvez et al., 2019, 2020). The combination of CaO with a NiO catalyst allows in-situ CO_2 removal (Florin et al., 2010; Lee et al., 2006) via the CO_2 adsorption reaction by CaO (eq. (2)).

CO_2 adsorption:

$$CO_2 + CaO \rightarrow CaCO_3 \Delta H^{\circ}_{298} = -178.8 \times 103 KJ/kmol \quad (2)$$

This route can be carried out at atmospheric pressure while producing high H_2 yields. Synthetic CaO-based sorbents, capable of absorbing CO_2, offer the potential to improve cost efficiency and future viability. CaO can increase the yield of H_2 from methane and biomass gasification through several pathways (Florin and Harris, 2008; Bunma and Kuchonthara, 2018). First, the CaO reacts directly with CO_2 to form $CaCO_3$, thereby isolating CO_2 and promoting a glycerol reaction to form a high selectivity of H_2 (Broda et al., 2012). To speed the conversion of biomass into hydrogen energy, a microwave-assisted blend is used NiO and catalyst (Shi et al., 2017). At 600 °C to 800 °C, the output of gaseous products ranged from 73% to 76% weight, with a hydrogen product reaching 55.7%. Microwave-assisted catalysis (MAC) is an efficient way to produce hydrogen from ethanol breakdown over sewage sludge catalyst residue. The power of the microwave has been increased from 300 to 560 W. Microwave heating has been proven to be significantly more effective than traditional heating. This ethanol conversions rate rose when microwave power was raised. At the ideal temperature, ethanol conversions can reach 98.4% (Deng et al., 2018).

Noble metal-based catalysts, which have high activity, are commonly employed to speed up the reaction rate of hydrogen synthesis (Sad et al., 2015; Husin et al., 2013). However, it has several drawbacks, such as promoting coke production at high temperatures (Medeiros et al., 2021). When compared to noble metals, nickel-based catalysts are the most promising, with a high level of activity and a modest price (Abdullah et al., 2017). Previously, we used NiO/zeolite catalyst for hydrogen generation via the water-glycerol system with microwave assistance, which reaches a conversion of 96.67% and H_2 selectivity of 73.5% (Husin et al., 2021). The active site in this study was NiO-supported zeolite (NiO/zeolite) catalysts. The presence of a catalyst along with CO_2 sorbent can reduce the reaction temperature and product purity during hydrogen production, thus supporting the reaction in Eq. (1). Therefore, the combination of nickel and CaO as CO_2 adsorbents provides a promising way to increase microwave efficiency in producing hydrogen production. In the presence of glycerol as a sacrificial electron donor, nickel acts as an active site, and CaO acts as CO_2 sorption resulting in considerably faster hydrogen generation from glycerol-water solution. Though microwave technologies have been examined for biofuel generation. The effect of the NiO/zeolite catalyst and CaO sorbent over microwave heating to produce hydrogen from water-glycerol mixtures has only been studied in a few research.

This work applied the inception wetness and wet mixing approach to combine NiO/zeolite and CaO to create nanocatalyst NiO/zeolite-CaO. Further, the effects of using a NiO/zeolite-CaO catalyst by microwave-assisted on the degradation hydrogen from a water-glycerol solution were investigated. The various methods, such as BET, XRD, and TEM, were used to characterize NiO/zeolite-CaO catalysts. The effect of microwave power and CaO loading on hydrogen production were studied systematically. The NiO/zeolite-CaO catalyst that was applied in this study has never been tested in microwave-assisted in the degradation hydrogen from a water-glycerol solution. Therefore, this work provides fundamental and important information in terms of the microwave setup in conjunction with NiO/zeolite-CaO catalysts and the effect of certain parameters on conversion and efficient selectivity of the glycerol reforming reaction in depth.

2. Experiments

2.1. Materials

Natural zeolite was taken from Aceh Besar Aceh Indonesia. Oxygen (O_2) and nitrogen (N_2) gases with a purity of 99.0% are obtained from one regional energy company. Distilled water was provided by the Chemical Engineering Laboratory staff. Glycerol ($C_3H_8O_3$) and Calcium oxide (CaO) was purchased from PT. Rudang Jaya Medan Company. Nickel nitrate (Ni $(NO_3)_2.6H_2O$), chloride acid (HCl), and silver nitrate ($AgNO_3$) were procured from Sigma-Aldrich and Merck and used as received.

2.2. Preparation of Nio/zeolite preparation

Natural zeolite was first cleaned of impurities attached to its surface. Furthermore, the zeolite is dried in a lower the amount of water in the oven. Natural zeolite was crushed, then passed through 53 μm. The powder was washed with distilled water, then dried at 120 °C. Zeolite activation was carried out by soaking it in a 3 M HCl solution. The combination was then filtered and rinsed with distilled water until it was neutral, and an $AgNO_3$ solution was used to conduct a negative test for the presence of Cl^-ions. Residue remained dry at a temperature for 120 °C to remove the water content. The dried zeolite was equalized in size by sifting to obtain a homogeneous size. The samples were labeled are acid-activated for zeolite natural.

NiO/zeolite catalysts containing 20 wt% Ni were prepared by inception wetness procedure using $Ni(NO_3)_2.6H_2O$ and natural zeolite (denoted: NiZ). The preparation procedure used is analogous to the previously reported (Husin et al., 2021). In brief, $Ni(NO_3)_2.6H_2O$ was first mixed in distilled water and then 2 g of zeolite was added while stirring vigorously. The catalyst was then dried in an oven for 12 h at 110 °C. To make nickel oxide, the nickel-loaded zeolite was calcined in the air at 600 °C for 2 h.

2.3. NiO/zeolite-CaO preparation

A wet mixing route mixed the NiO/zeolite and CaO sorbents. The CaO content of the NiO/zeolite was 10 wt.%, 30 wt.%, 40 wt.%, 50 wt.%, 60 wt.%, and 100 wt.%. Commercial CaO were first calcined at 800 °C for 3 h. The necessary molar ratios of CaO and NiO/zeolite were combined in deionized water for the wet mixed catalyst-sorbents, then encouraged with vigorous stirring by magnetic stirrer for 6 h. The resulting mixtures were dried in an oven at 110 °C for 12 h, then fully ground and calcined at the temperature of 700 °C in nitrogen for three h. Finally, the powder was dried and stored in a glass bottle using a desiccator. The catalyst with CaO content of 10 wt.%, 30 wt.%, 40 wt.%, 50 wt.%, 60 wt.%, and 100 wt.% are denoted as NiZ-Ca10, NiZ-Ca30, NiZ-Ca50, NiZ-Ca60, and Ca-100.

2.4. Catalyst characterization

Micromeritics ASAP automatic absorptiometer was applied for measurements of the surface area and porosity of the catalyst using liquid nitrogen as adsorbent at 196 °C. The specific BET surface area has been calculated from the nitrogen adsorption isotherm. Using a Philips X'pert diffraction-meter and Cu K (= 0.154 nm) produced at 40 kV and 20 mA, the composition of the NiO/zeolite-CaO catalyst-sorbents was investigated. The microstructures of materials were discovered using a transmission electron microscope (TEM, JEOL 2010 TEM equipment) at Universitas Gadjah Mada in Indonesia.

2.5. Experimental apparatus and procedure

A microwave was used to catalyze the conversion of aqueous glycerol to hydrogen in a fixed bed reactor. Fig. 1 shows a schematic diagram of the equipment. In the microwave oven, a quartz glass reactor (40 cm long, 1.0 cm in diameter) packed with 1 g of catalyst was placed.. The microwave reactor continuous output can be set manually at with power of 300–600 W. To investigate the influence of CaO/NiO ratio and microwave heating on conversion and hydrogen selectivity, feed flow rates were fixed at 0.5 ml/min. In the reactor, 1:10 liquid glycerol water was introduced. A micro-syringe was used to precisely control the flow rate of glycerol. The air inside the reactor was evacuated before the microwave commenced by using gas as a gas mixture.

The output gas was collected using a gasbag on a regular basis and analyzed using a Shimadzu GC-8A gas chromatograph with a thermal conductivity detector (TCD) and a mole sieve 5 A column.

3. Results and discussion

3.1. Characterizations of catalyst

3.1.1. BET catalyst surface area analysis

Characterization of the catalyst was analyzed by surface area analyzer (SAA) instrumentation while using the BET method. This analysis is intended to determine the surface area of the catalyst. SAA characterization results are shown in **Table 1**.

As depicted in **Table 1**, the surface area of the NiO/zeolite catalyst obtained was 53.39 m^2/g. By adding CaO on the NiO/zeolite, the surface increased to 102.49 m^2/g. The pore volume and the average pore diameter did not significantly differ between NiO/zeolite and NiO/zeolite. CaO. The addition of CaO resulted in a significant increase in the specific surface area of the catalyst as well as a decrease in pore volume and pore size. A high surface area provided a large contact area between the molecules of the reactants with the catalyst. The magnitude of the contact directly affected the process of catalysis, and reactant molecules moved freely on the surface of the activated catalyst and reacted to the products. The surface area of the catalyst affected the activity of the catalyst. Increasing the surface area of the catalyst spreads more active phase so hydrogen gas production increases.

Table 1
BET catalyst surface area analysis.

catalyst	Surface area (m^2/g)	Pore volume (cm^3/g)	Average pore diameter (nm)
NiO/zeolite	53.39	0.37	9.72
NiO/zeolite. CaO	102. 49	0.31	14.78

3.1.2. Diffractometer analysis for X-ray (XRD)

The XRD patterns of natural zeolite, NiO/zeolite, and NiO/zeolite-CaO are shown in Fig. 2. As can be seen in Fig. 2a.1, the characteristic peaks of natural zeolite (Z) indicate the type of clinoptilolite. Meanwhile, the pattern demonstrates the production of a crystalline phase indexed by a single cubic phase (NiO) and a natural zeolite phase after impregnating nickel compounds on the surface of natural zeolite; crystallized metal impurities were identified the diffractogram (Fig. 2a.2). Compared with the XRD of single zeolite (Fig. 2a.1) and NiO/zeolite catalyst (Fig. 2a.2), the structure of natural zeolite did not change significantly, indicating that zeolite is more thermally stable. The peaks at 37.21°, 43.24°, and 62.81° correspond to the NiO crystal faces (111) and (200), respectively, and reflect the creation of a nickel phase characteristic. The presence of NiO upon this surface of zeolite could be due to the catalyst's greater activity in hydrogen generation (H. Husin et al., 2011).

Fig. 2.b confirms that the phase of CaO can be indexed through all the peaks with an Fm-3 m space group. From XRD analysis indicated the diffraction peaks at 29.3°, 34.1°, 38.7°, and 54.2° corresponding to (110), (111), (200), and (211) plane, which were in agreement with the JCPDS data (JCPDS: 82–1691) for CaO particles (Balázsi et al., 2007). The narrow and high intense peaks define the crystalline structure of the CaO catalyst. Debye Scherrer's formula was used to calculate the mean crystallite size. (Patterson, 1939).

$$Size\ of\ crystallite = (0.94\lambda / (FWHM{\cdot}Cos\theta)) \quad (3)$$

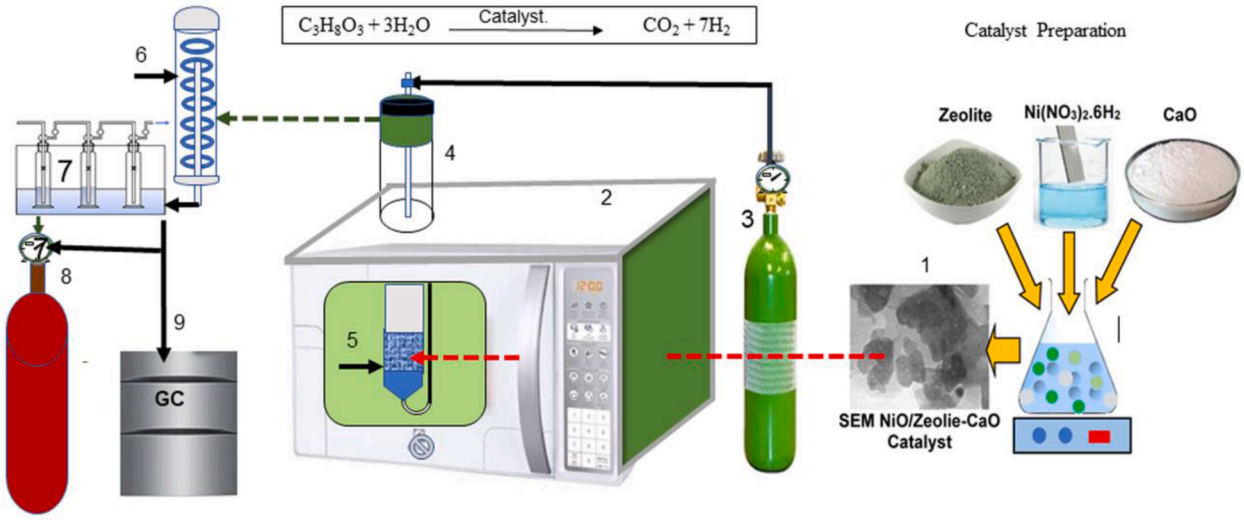

Fig. 1. Experimental setup of catalytic reactor microwave-assisted of hydrogen from glycerol-water solution 1. SEM of NiO/zeolite-CaO catalyst; 2. Microwave oven; 3. N2 gas; 4. Quartz glass reactor; 5. NiO/zeolite-CaO catalyst; 6. Condenser; 7. Absorption solution; 8. Gas product; 9. Gas chromatography.

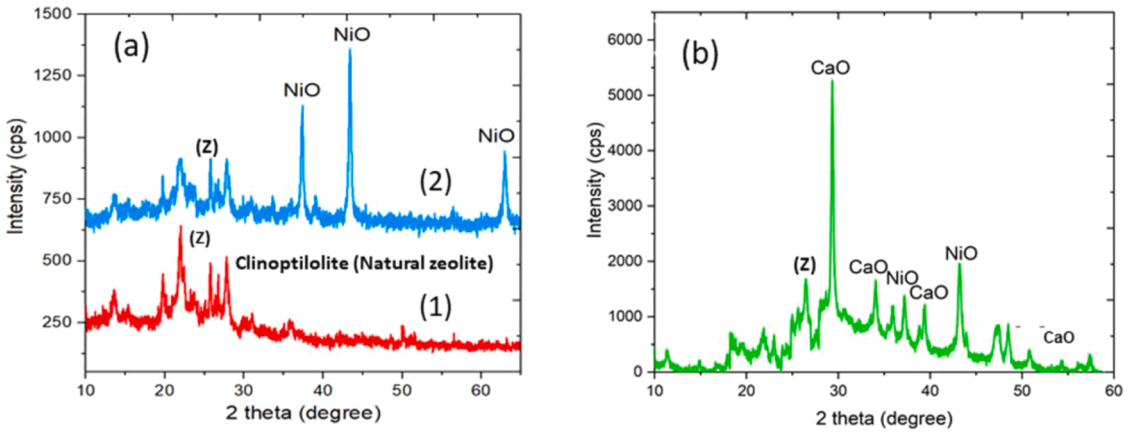

Fig. 2. XRD patterns of (2a.1) Natural zeolite (Z) (2a.2) NiO/zeolite (NiZ). (2b) NiO/zeolite-CaO (NiZ-Ca).

Where X-ray wavelength is 1.54, FWHM is the broadening of the diffracted peak at half maximum, and is the corresponding Bragg angle, which the means crystalline size is 15 nm corresponding to plane (110) is shown in Fig. 2b. The presence of CaO in the catalyst is expected to increase the surface area of the catalyst as shown in BET data. Increasing the surface area of the catalyst is expected to increase the conversion of the glycerol and hydrogen generation by the absorption of CO2 from the reaction products (Eq. (2)).

3.1.3. Analysis using a transmission electron microscope (TEM)

The morphology of the NiO/zeolite and NiO/zeolite-CaO catalysts are recorded by Transmission electron microscopy (TEM), as shown in **Fig. 3**. Both the NiO/zeolite and NiO/zeolite-CaO possessed a nano-structured morphology.

The picture in Fig. 3.a the dispersion of NiO species across the full surface of the zeolite support is plainly visible. with the particles size is in the range of 30–150 nm. It also depicted that NiO particle sizes are around 4–6 nm, due to the wide surface area, there is a great dispersion, as confirmed by the BET data. Meanwhile, from Fig. 3.b, it can be seen that the particle size of the NiO/zeolite-CaO looks smaller and more regular in shape. The uniform dispersion of NiO/zeolite, providing a stable nano-sized framework for the CaO grains contributes to the improvement of the thermal stability of the catalyst (Arif et al., 2019). Crystallite also call grains, as far as material science is concerned, refer to that volume of material within which the crystal structure and the orientation of the crystals are the same. Particle size, on the other hand, is a macro phenomenon. It is the size of the particles, which may have one or several grains within them. It is impossible to have a grain with multiple particles because the smallest thing we could have would always represent one.

The particle sizes of NiO/zeolite-CaO are around 15–80 nm, which indicates that CaO could reduce agglomeration during the heating process. Accordingly, the specific surface area, pore-volume, and pore diameter of the NiO/zeolite catalyst with and without CaO content are presented in Table 1. It can be seen that the addition of CaO resulted in an increase in particle size, specific surface area, and catalyst pore volume. NiO/zeolite.CaO samples showed smaller particle sizes (from XRD and TEM analysis), namely 15–80 nm, and larger specific surface areas (102.49 m^2/g). This can mainly be attributed to the blocking of the mesoporous moiety of the catalyst and the structural change of NiO and zeolite through their interaction with CaO. Furthermore, the pore diameter and particle size of the catalyst change. Smaller particle sizes and higher surface area will contribute to increased glycerol conversion and hydrogen selectivity. Furthermore, the NiO species must be widely

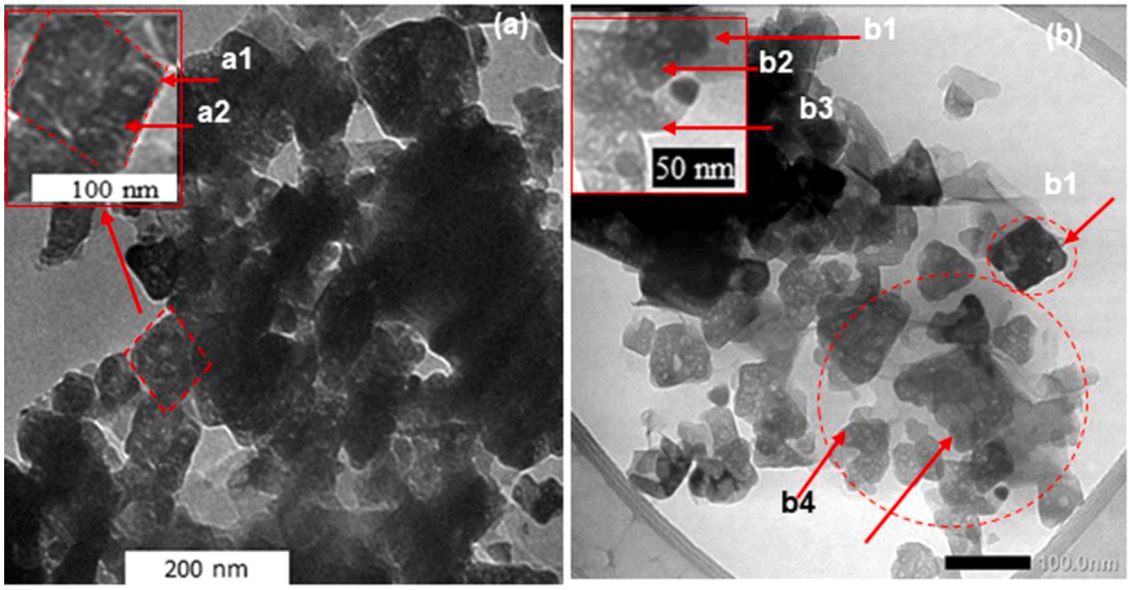

Fig. 3. TEM images of (a) NiO/zeolite catalyst (insert picture: (a1 view of zeolite, a2 view of NiO; and (b) NiO/zeolite-CaO catalyst (insert picture: b1 view of zeolite, b2 view of NiO, b3 view of CaO, b4 view NiO/zeolite-CaO).

spread across the support's surface.

3.2. Glycerol degradation catalytic tests

3.2.1. At various microwave powers, the effect of CaO loading on glycerol-water conversion

The NiO/zeolite-CaO catalyst performance was investigated in a fixed bed reactor at 300–600 W. The effect of CaO content and microwave power on glycerol conversion is presented in **Fig. 4**. It can be seen that the conversion of glycerol on NiZ at a power of 600 W reached 96.67%. The conversion increased slightly by adding 10%, 30%, and 50% CaO on NiO/zeolite, respectively.

The highest glycerol conversion was achieved 98,6% by applying NiZ-Ca50 catalyst. Further increase in the amount of CaO loading did not show an increase in the glycerol conversion value. Excessive loading of CaO can also result in the agglomeration of NiO/zeolite and CaO nanoparticles and weaken the function of the catalyst (Nahil et al., 2013). Even when using 100% CaO, the glycerol conversion goes to lower conversion, as shown in Fig. 4. This fact is possible because CaO mainly acted as a sorbent and did not function as an active phase for the reaction of breaking glycerol into hydrogen (H. Husin et al., 2017). It is well known that NiO is a suitable active site to catalyze glycerol-water reaction at moderate-higher temperatures (Dou et al., 2021). Moreover, NiO support by zeolite has demonstrated a higher level of commitment to the glycerol reaction at 600 W than other oxides such as Rh/Al2O3, CeO2, MgO oxides (Charisiou et al., 2020). While the increase in microwave power was followed by an increase in glycerol conversion. This phenomenon can be caused by a rise in heating rate as it could increase the temperature inside of the reactor. Higher temperatures could cause an increase in conversions. This might be due to a higher temperature; it produces more energy and could accelerate the reaction rate (Adhikari et al., 2009).

3.2.2. The effect of CaO loading on hydrogen produced at various microwave powers

The hydrogen production from the degradation reactions of glycerol over NiO/zeolite-CaO at different CaO sorbent was investigated at an MW power of 300–600 W and 20 wt.% NiO loading on zeolite surface. As demonstrated in **Fig. 5**, hydrogen generation increases with increasing microwave power at different CaO loading. Ni/Z had the lowest H_2 generation. In addition, the hydrogen generation on NiO/zeolite-CaO, at 600 W, reaches of 93%, 96%, 96.6%, and 96.3%, at CaO loading 10%, 30%, 50%, and 60%, respectively. In contrast, the CO_2 decreased from 17% into 3%, 2%, and finally was almost undetectable. It's probably because of the role of CaO act as absorbing CO_2 (Broda et al., 2012).

It is also suggested the NiO/zeolite-CaO catalyst revealed better catalytic performance. The MW power has played a crucial role in the microwave catalysis process. Moreover, combining CaO with NiO/zeolite catalyst led to an increase in surface-active reaction site of the nanomaterials, also larger it's surface of CO_2 sorption. This finding is in agreement with those reported by other research groups (Serra et al., 2020).

3.2.3. Effect of CaO and nickel loading on hydrogen generation at microwave power 600 W

Fig. 6 reported that the best conditions were achieved at a microwave power of 600 W, a feed flow rate of 0.5 ml/min, 50% CaO, and 20% NiO content to increase the glycerol conversion and the highest H_2 purity. In this condition, the best performance is NiZ-Ca50 catalyst with glycerol conversion reached 98.8% and H_2 generation 96.6%.

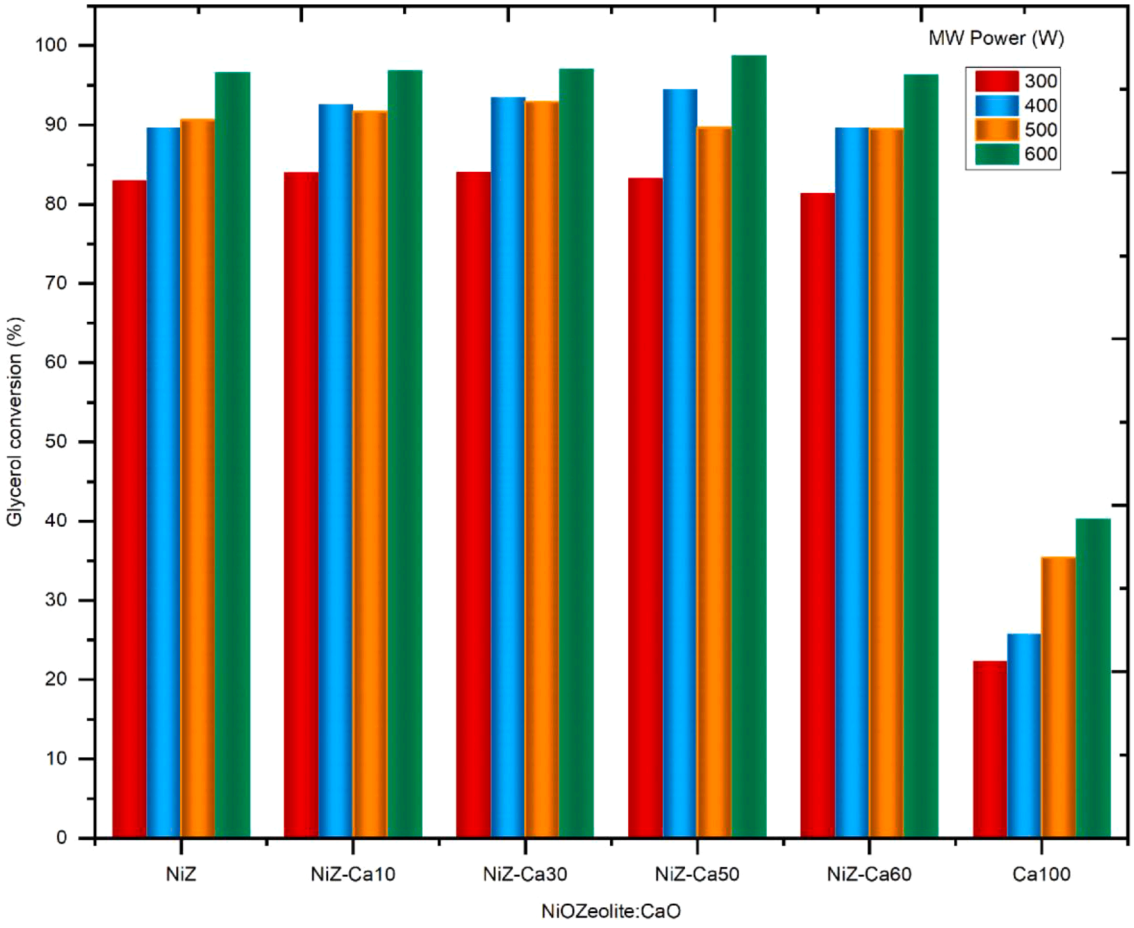

Fig. 4. Glycerol conversion at different CaO loading and microwave power.

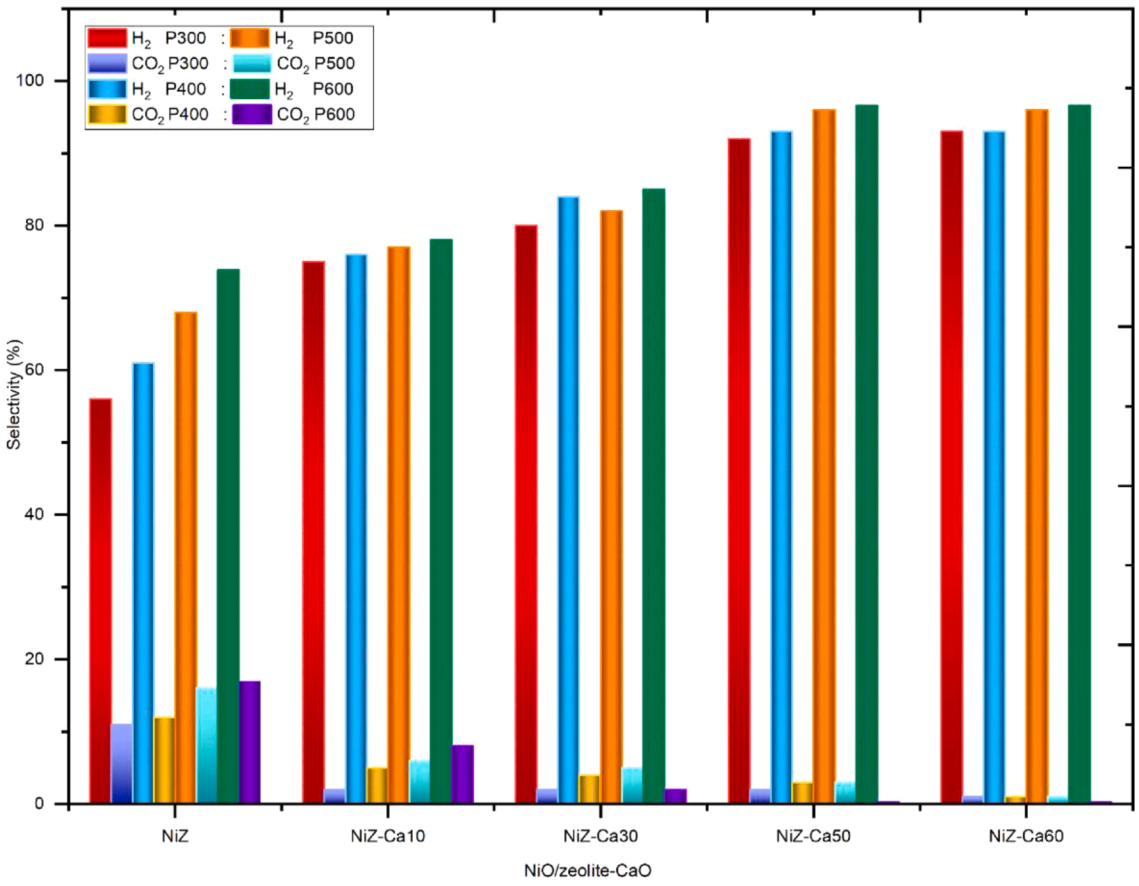

Fig. 5. Product selectivity at different CaO loading and microwave power.

Surprisingly, combining the NiO catalyst on zeolite support and CaO sorbent results in a significant improvement in the microwave catalytic hydrogen production activity of NiO/zeolite-CaO. As evident in BET and TEM data, adding CaO to the catalyst cause its surface area to increase and more regular in shape. The uniform dispersion of nickel particles will contribute to increased glycerol conversion and hydrogen selectivity. The larger surface area gives the reactants better access to the nickel/zeolite and CaO sites, those increasing the reaction rate, which can facilitate CO_2 molecules to be further adsorbed (Nimmas et al., 2020). Our result is in good agreement with the result observed by Luo et al. (2015) that the adsorption capacity of CO_2 is correlated with the amount of CaO and NiO catalyst in the sorbent mixture. The NiO/Ni-$NiAl_2O_4$.CaO catalyst was applied for glycerol steam reforming with and without in-situ CO_2 removal at 500 °C and 600 °C. The purity of hydrogen from steam reforming glycerol was reached 96.1% (Dou et al., 2013), whereas the conversion and hydrogen selectivity by reforming of glycerol over *Re*/Ni-CaO catalyst of 62% and 56%, respectively(Arif et al., 2019).

The NiO/zeolite-CaO catalyst appears to be a superior contender for hydrogen production by microwave-assisted catalytic irradiation of glycerol-water solution than the previous studies mentioned. In addition, the synergic effect of NiO/zeolite active site, CaO sorbent act as CO_2 sorption, and microwave irradiation which provides activation energy for the reaction, resulting in an effective hydrogen catalysis process. The interaction between microwave irradiation, nickel catalyst particles, CaO sorbent could result in electrostatic discharge, leading to the formation of active sites in the reaction medium (Cai et al., 2018; Raso et al., 2021).

4. Conclusion

Synthesis of NiO/zeolite-CaO catalyst prepared by inception wetness and wet mixing has succeeded and application on the microwave-assisted irradiation in the rapid synthesis of glycerol-to-hydrogen production. The properties and performance of NiO/zeolite-CaO were better influenced by the content of NiO, CaO, and microwave power to accelerate glycerol conversion and hydrogen selectivity. The synergic effect between microwave power of 600 W, under the action of NiZ-Ca50 catalyst, achieved glycerol conversion of 98.8% and hydrogen selectivity of 96.7%. The NiO/zeolite and CaO-modification under 600 W can be used as a candidate material for conversion glycerol-water solution on microwave heating to produce hydrogen. Thus, the synergetic effect between NiO/zeolite active site, CaO sorbent act as CO_2 sorption, via microwave-assisted irradiation resulted in a significant enhancement of the catalytic glycerol conversion and the hydrogen generation.

CRediT author statement

Husni Husin: Conceptualization, Supervision, Methodology, Writing-Original draft. **Erdiwansyah:** Writing-Original draft, Reviewing and Editing. **Ahmadi:** Investigation, Collecting Data, Formal Analysis. **Fahrizal Nasution:** Investigation, Formal Analysis, Collecting Data. **Wahyu Rinaldi:** Validation, Writing-Review & Editing. **Faisal Abnisa:** Writing-Review & Editing, Validation. **Rizalman Mamat:** Validation.

Declaration of Competing Interest

The authors declare that they have no known competing financial

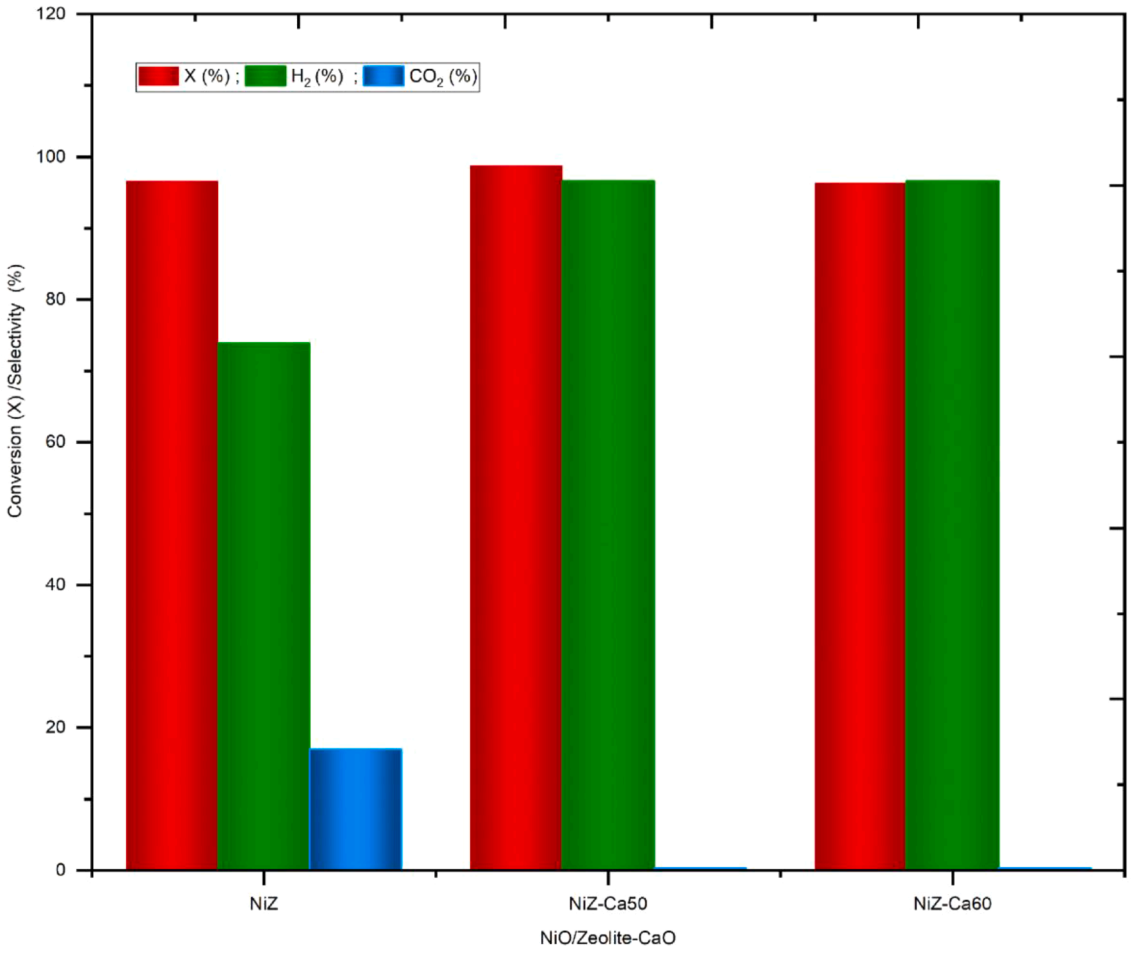

Fig. 6. Conversion and selectivity at microwave power 600 W.

interests or personal relationships that could have appeared to influence the work reported in this paper.

Acknowledgement

This research is funded by the Indonesian Ministry of Higher Education and Technology under the grant of University Leading Basic Research (PDUPT) 2021 (Contract No. 056/E41/AK04PT/2021). In addition, the World Class Professor Program (Scheme-B) in 2021 (Contract No. 2637/E4/KK.04.05/2021) from the Indonesian Ministry of Education, Culture, Research, and Technology Indonesia (Kemdikbudristek) has enabled the authors to consult with Prof. Rizalman Mamat from University Malaysia Pahang to complete the writing of this paper

References

Abdel-Basset, M., Gamal, A., Chakrabortty, R.K., Ryan, M.J., 2021. Evaluation of sustainable hydrogen production options using an advanced hybrid MCDM approach: a case study. Int. J. Hydrogen Energy 46 (5), 4567–4591. https://doi.org/10.1016/j.ijhydene.2020.10.232.

Abdullah, B., Abd Ghani, N. A., & Vo, D.V.N. (2017). Recent advances in dry reforming of methane over Ni-based catalysts. J. Clean. Prod., 162, 170–185, 10.1016/j.jclepro.2017.05.176.

Adhikari, S., Fernando, S.D., Haryanto, A., 2009. Hydrogen production from glycerol: an update. Energy Convers. Manag. 50 (10), 2600–2604. https://doi.org/10.1016/j.enconman.2009.06.011.

Al Bacha, S., Thienpont, A., Zakhour, M., Nakhl, M., Bobet, J.-L, 2021. Clean hydrogen production by the hydrolysis of magnesium-based material: effect of the hydrolysis solution. J. Clean. Prod. 282, 124498 https://doi.org/10.1016/j.jclepro.2020.124498.

Aparamarta, H.W., Gunawan, S., Husin, H., Azhar, B., Tri Aditya, H., 2020. The effect of high oleic and linoleic fatty acid composition for quality and economical of biodiesel from crude Calophyllum inophyllum oil (CCIO) with microwave-assisted extraction (MAE), batchwise solvent extraction (BSE), and combination of MAE–BSE methods. Energy Rep. 6, 3240–3248. https://doi.org/10.1016/j.egyr.2020.11.197.

Arif, N.N.M., Abidin, S.Z., Osazuwa, O.U., Vo, D.V.N., Azizan, M.T., Taufiq-Yap, Y.H., 2019. Hydrogen production via CO_2 dry reforming of glycerol over ReNi/CaO catalysts. Int. J. Hydrogen Energy 44 (37), 20857–20871.

Baloyi, L.N., North, B.C., Langmi, H.W., Bladergroen, B.J., Ojumu, T.V., 2016. The production of hydrogen through the use of a 77 wt% Pd 23 wt% Ag membrane water gas shift reactor. S. Afr. J. Chem. Eng. 22, 44–54. https://doi.org/10.1016/j.sajce.2016.11.001.

Broda, M., Kierzkowska, A.M., Baudouin, D., Imtiaz, Q., Coperet, C., Muller, C.R., 2012. Sorbent-enhanced methane reforming over a Ni–Ca-based, bifunctional catalyst sorbent. ACS Catal. 2 (8), 1635–1646.

Bunma, T., Kuchonthara, P., 2018. Synergistic study between CaO and MgO sorbents for hydrogen rich gas production from the pyrolysis-gasification of sugarcane leaves. Process Saf. Environ. Prot. 118, 188–194. https://doi.org/10.1016/j.psep.2018.06.034.

Cai, F., Pan, D., Ibrahim, J.J., Zhang, J., Xiao, G., 2018. Hydrogenolysis of glycerol over supported bimetallic Ni/Cu catalysts with and without external hydrogen addition in a fixed-bed flow reactor. Appl. Catal. A: Gen. 564, 172–182. https://doi.org/10.1016/j.apcata.2018.07.029.

Can, E., Yildirim, R., 2019. Data mining in photocatalytic water splitting over perovskites literature for higher hydrogen production. Appl. Catal. B: Environ. 242, 267–283. https://doi.org/10.1016/j.apcatb.2018.09.104.

Charisiou, N.D., Italiano, C., Pino, L., Sebastian, V., Vita, A., Goula, M.A., 2020. Hydrogen production via steam reforming of glycerol over $Rh/\gamma\text{-}Al_2O_3$ catalysts modified with CeO_2, MgO or La_2O_3. Renew. Energy 162, 908–925. https://doi.org/10.1016/j.renene.2020.08.037.

Chehade, G., Lytle, S., Ishaq, H., Dincer, I., 2020. Hydrogen production by microwave based plasma dissociation of water. Fuel 264, 116831. https://doi.org/10.1016/j.fuel.2019.116831.

Czylkowski, D., Hrycak, B., Jasiński, M., Dors, M., Mizeraczyk, J., 2016. Microwave plasma-based method of hydrogen production via combined steam reforming of methane. Energy 113, 653–661. https://doi.org/10.1016/j.energy.2016.07.088.

Deng, W., Liu, S., Ma, J., Su, Y., 2018. Microwave-assisted ethanol decomposition over pyrolysis residue of sewage sludge for hydrogen-rich gas production. Int. J.

Hydrogen Energy 43 (33), 15762–15772. https://doi.org/10.1016/j.ijhydene.2018.07.067.
Dou, B., Wang, C., Chen, H., Song, Y., Xie, B., 2013. Continuous sorption-enhanced steam reforming of glycerol to high-purity hydrogen production. Int. J. Hydrogen Energy 38 (27), 11902–11909. https://doi.org/10.1016/j.ijhydene.2013.07.026.
Dou, B., Zhao, L., Zhang, H., Wu, K., Zhang, H., 2021. Renewable hydrogen production from chemical looping steam reforming of biodiesel byproduct glycerol by mesoporous oxygen carriers. Chem. Eng. J. 416, 127612 https://doi.org/10.1016/j.cej.2020.127612.
Florin, N.H., Harris, A.T., 2008. Screening CaO-based sorbents for CO2 capture in biomass gasifiers. Energy Fuels 22 (4), 2734–2742. https://doi.org/10.1021/ef700751g.
Florin, N.H., Blamey, J., Fennell, P.S., 2010. Synthetic CaO-based sorbent for CO2 capture from large-point sources. Energy Fuels 24 (8), 4598–4604.
Hani, M.R., Mahidin, M., Husin, H., Hamdani, H., & Khairil, K. (2018). Oil palm biomass utilization as an energy source and its possibility use for polygeneration scenarios in Langsa City, Aceh Province, Indonesia. IOP Conference Series: Materials Science and Engineering, 334(1), 12003. doi:10.1088/1757-899X/334/1/012003.
Husin, H., Chen, H.M., Su, W.N., Pan, C.J., Chuang, W.T., Sheu, H.S., Hwang, B.J., 2011a. Green fabrication of La-doped $NaTaO_3$ via H_2O_2 assisted sol–gel route for photocatalytic hydrogen production. Appl. Catal. B: Environ. 102 (1–2), 343–351. https://doi.org/10.1016/j.apcatb.2010.12.024.
Husin, H., Su, W.N., Chen, H.M., Pan, C.J., Chang, S.H., Rick, J., Chuang, W.T., Sheu, H.S., & Hwang, B.J. (2011). Photocatalytic hydrogen production on nickel-loaded LaxNa1−xTaO3 prepared by hydrogen peroxide-water based process. Green Chemistry, 13(7), 1745–1754. 10.1039/C1GC15070G.
Husin, H., Su, W.N., Pan, C.J., Liu, J.Y., Rick, J., Yang, S.C., Chuang, W.T., Sheu, H.S., Hwang, B.J., 2013. Pd/NiO core/shell nanoparticles on La0.02Na0.98TaO3 catalyst for hydrogen evolution from water and aqueous methanol solution. Int. J. Hydrogen Energy 38 (31), 13529–13540. https://doi.org/10.1016/j.ijhydene.2013.07.116.
Husin Komala; Sy, Yuliana; Syawaliah, S.; Saisa, S., H. P. (2014). Synthesis of nanocrystalline of lanthanum doped NaTaO3 and photocatalytic activity for hydrogen production. J. Eng. Technol. Sci., Vol 46, No 3 (2014), 318–327. http://journals.itb.ac.id/index.php/jets/article/view/881.
Husin, H., Adisalamun, Sy, Y., Asnawi, T. M., & Hasfita, F. (2017). Pt nanoparticle on La0.02Na0.98TaO3 catalyst for hydrogen evolution from glycerol aqueous solution. AIP Conf. Proc., 1788(1), 30073. 10.1063/1.4968326.
Husin, H., Pontas, K., Yunardi, Adisalamun, Alam, P.N., Hasfita, F, 2017b. Photocatalytic hydrogen production over Ni/La-NaTaO3 nanoparticles from NaCl-water solution in the presence of glucose as electron donor. ASEAN J. Chem. Eng. 17 (2), 27–36. https://doi.org/10.22146/ajche.49553.
Husin, H., Asnawi, T.M., Firdaus, A., Husaini, H., Ibrahim, I., Hasfita, F., 2018. Solid catalyst nanoparticles derived from oil-palm empty fruit bunches (OP-EFB) as a renewable catalyst for biodiesel production. IOP Conf. Ser.: Mater. Sci. Eng. 358 (1), 12008.
Husin, H., Mahidin, M., Pontas, K., Ahmadi, A., Ridho, M., Erdiwansyah, E., Nasution, F., Hasfita, F., Hussin, M.H., 2021. Microwave-assisted catalysis of water-glycerol solutions for hydrogen production over NiO/zeolite catalyst. Heliyon 7 (7), e07557. https://doi.org/10.1016/j.heliyon.2021.e07557.
Khodabandehloo, M., Larimi, A., & Khorasheh, F. (2020). Comparative process modeling and techno-economic evaluation of renewable hydrogen production by glycerol reforming in aqueous and gaseous phases. Energy Conversion and Management, 225, 113483. 10.1016/j.enconman.2020.113483.
Kasirajan, R., 2021. Biodiesel production by two step process from an energy source of Chrysophyllum albidum oil using homogeneous catalyst. S. Afr. J. Chem. Eng. 37, 161–166. https://doi.org/10.1016/j.sajce.2021.05.011.
Koc, S., Avci, A.K., 2017. Reforming of glycerol to hydrogen over Ni-based catalysts in a microchannel reactor. Fuel Process. Technol. 156, 357–365. https://doi.org/10.1016/j.fuproc.2016.09.019.
Lee, D.K., Hyun Baek, I. I., & Lai Yoon, W. (2006). A simulation study for the hybrid reaction of methane steam reforming and in situ CO2 removal in a moving bed reactor of a catalyst admixed with a CaO-based CO2 acceptor for H2 production. Int. J. Hydrogen Energy, 31(5), 649–657, 10.1016/j.ijhydene.2005.05.008.
Lin, Y.C., 2013. Catalytic valorization of glycerol to hydrogen and syngas. Int. J. Hydrogen Energy 38 (6), 2678–2700. https://doi.org/10.1016/j.ijhydene.2012.12.079.
Luo, C., Zheng, Y., Xu, Y., Ding, N., Shen, Q., Zheng, C., 2015. Wet mixing combustion synthesis of CaO-based sorbents for high temperature cyclic CO2 capture. Chem. Eng. J. 267, 111–116. https://doi.org/10.1016/j.cej.2015.01.005.
Macedo, M.S., Soria, M.A., Madeira, L.M., 2019. Glycerol steam reforming for hydrogen production: traditional versus membrane reactor. Int. J. Hydrogen Energy 44 (45), 24719–24732. https://doi.org/10.1016/j.ijhydene.2019.07.046.
Mardian, R., Husin, H., Pontas, K., Zaki, M., Asnawi, T.M., Ahmadi, 2018. Hydrogen production from water-glucose solution over NiO/La-NaTaO3 photocatalyst. IOP Conf. Ser.: Mater. Sci. Eng. 334, 12013. https://doi.org/10.1088/1757-899x/334/1/012013.
Medeiros, R.L.B.A., Figueredo, G.P., Macedo, H.P., A.S, Oliveira, Â., Rabelo-Neto, R.C., Melo, D.M.A., Braga, R.M., Melo, M.A.F, 2021. One-pot microwave-assisted combustion synthesis of Ni-Al2O3 nanocatalysts for hydrogen production via dry reforming of methane. Fuel 287, 119511. https://doi.org/10.1016/j.fuel.2020.119511.
Moran, M.J., Martina, K., Stefanidis, G.D., Jordens, J., Gerven, T.Van, Goovaerts, V., Manzoli, M., Groffils, C., Cravotto, G, 2020. Glycerol: an optimal hydrogen source for microwave-promoted Cu-catalyzed transfer hydrogenation of nitrobenzene to aniline. Front. Chem. 8, 34.
Nahil, M.A., Wang, X., Wu, C., Yang, H., Chen, H., Williams, P.T., 2013. Novel bi-functional Ni-Mg-Al-CaO catalyst for catalytic gasification of biomass for hydrogen production with in situ CO_2 adsorption. Rsc Advance 3 (16), 5583–5590.
Nimmas, T., Wongsakulphasatch, S., Kui Cheng, C., Assabumrungrat, S., 2020. Bi-metallic CuO-NiO based multifunctional material for hydrogen production from sorption-enhanced chemical looping autothermal reforming of ethanol. Chem. Eng. J. 398, 125543 https://doi.org/10.1016/j.cej.2020.125543.
Parvez, A.M., Afzal, M.T., Jiang, P., Wu, T., 2020. Microwave-assisted biomass pyrolysis polygeneration process using a scaled-up reactor: product characterization, thermodynamic assessment and bio-hydrogen production. Biomass and Bioenergy 139, 105651. https://doi.org/10.1016/j.biombioe.2020.105651.
Parvez, A.M., Wu, T., Afzal, M.T., Mareta, S., He, T., Zhai, M., 2019. Conventional and microwave-assisted pyrolysis of gumwood: a comparison study using thermodynamic evaluation and hydrogen production. Fuel Process. Technol. 184, 1–11. https://doi.org/10.1016/j.fuproc.2018.11.007.
Patterson, A.L., 1939. The Scherrer formula for X-ray particle size determination. Physical Review 56 (10), 978.
Qingli, X., Zhengdong, Z., Kai, H., Shanzhi, X., Chuang, M., Chenge, C., Huan, Y., Yang, Y., Yongjie, Y., 2021. Ni supported on MgO modified attapulgite as catalysts for hydrogen production from glycerol steam reforming. Int. J. Hydrogen Energy 46 (54), 27380–27393. https://doi.org/10.1016/j.ijhydene.2021.06.028.
Raso, R., García, L., Ruiz, J., Oliva, M., Arauzo, J., 2021. Aqueous phase hydrogenolysis of glycerol over Ni/Al-Fe catalysts without external hydrogen addition. Appl. Catal. B: Environ. 283, 119598 https://doi.org/10.1016/j.apcatb.2020.119598.
Ribao, P., Alexandra Esteves, M., Fernandes, V. R., Rivero, M.J., Rangel, C.M., & Ortiz, I. (2019). Challenges arising from the use of TiO2/rGO/Pt photocatalysts to produce hydrogen from crude glycerol compared to synthetic glycerol. Int. J. Hydrogen Energy, 44(53), 28494–28506, 10.1016/j.ijhydene.2018.09.148.
Sad, M.E., Duarte, H.A., Vignatti, C., Padró, C.L., Apesteguía, C.R., 2015. Steam reforming of glycerol: hydrogen production optimization. Int. J. Hydrogen Energy 40 (18), 6097–6106. https://doi.org/10.1016/j.ijhydene.2015.03.043.
Serra, J.M., Borrás-Morell, J.F., García-Baños, B., Balaguer, M., Plaza-González, P., Santos-Blasco, J., Catalán-Martínez, D., Navarrete, L., Catalá-Civera, J.M., 2020. Hydrogen production via microwave-induced water splitting at low temperature. Nat. Energy 5 (11), 910–919.
Sharma, Y.C., Kumar, A., Prasad, R., Upadhyay, S.N., 2017. Ethanol steam reforming for hydrogen production: latest and effective catalyst modification strategies to minimize carbonaceous deactivation. Renew. Sustain. Energy Rev. 74, 89–103. https://doi.org/10.1016/j.rser.2017.02.049.
Shi, K., Yan, J., Luo, X., Lester, E., & Wu, T. (2017). Microwave-assisted pyrolysis of bamboo coupled with reforming by activated carbon for the production of hydrogen-rich syngas. Energy Procedia, 142, 1640–1646 10.1016/j.egypro.2017.12.543.
Sui, J., Chen, Z., Wang, C., Wang, Y., Liu, J., Li, W., 2020. Efficient hydrogen production from solar energy and fossil fuel via water-electrolysis and methane-steam-reforming hybridization. Appl. Energy 276, 115409. https://doi.org/10.1016/j.apenergy.2020.115409.
Sy, Y., Nurhazanah, N., Maulana, A., Mahidin, M., Husin, H., 2019. Study of pH influences on the performance of Na-loaded $NbOPO_4$ solid acid catalyst for biofuel production. J. Phys. Conf. Ser. 1402 (5), 55006. https://doi.org/10.1088/1742-6596/1402/5/055006.
Tamošiūnas, A., Valatkevičius, P., Gimžauskaitė, D., Valinčius, V., Jeguirim, M., 2017. Glycerol steam reforming for hydrogen and synthesis gas production. Int. J. Hydrogen Energy 42 (17), 12896–12904. https://doi.org/10.1016/j.ijhydene.2016.12.071.
Wang, L.qun, Dun, Y.huan, Xiang, X.nan, Jiao, Z.jing, Zhang, T.qing, 2011. Thermodynamics research on hydrogen production from biomass and coal co-gasification with catalyst. Int. J. Hydrogen Energy 36 (18), 11676–11683. https://doi.org/10.1016/j.ijhydene.2011.06.064.
Widyawati, M., Church, T.L., Florin, N.H., Harris, A.T., 2011. Hydrogen synthesis from biomass pyrolysis with in situ carbon dioxide capture using calcium oxide. Int. J. Hydrogen Energy 36 (8), 4800–4813. https://doi.org/10.1016/j.ijhydene.2010.11.103.
Zhao, C., Yang, L., Xing, S., Luo, W., Wang, Z., Lv, P., 2018. Biodiesel production by a highly effective renewable catalyst from pyrolytic rice husk. J Clean Prod 199, 772–780. https://doi.org/10.1016/j.jclepro.2018.07.242.
Zou, J., Oladipo, J., Fu, S., Al-Rahbi, A., Yang, H., Wu, C., Cai, N., Williams, P., & Chen, H. (2018). Hydrogen production from cellulose catalytic gasification on CeO2/Fe2O3 catalyst. Energy Convers. Manag., 171, 241–248, 10.1016/j.enconman.2018.05.104.